# Methodology for Numerical Simulation of Trabecular Bone Structures Mechanical Behavior

**M.A. Argenta[1], A.P. Gebert[2], E.S. Filho[3], B.A. Felizari[4] and M.B. Hecke[5]**

**Abstract:** Various methods in the literature proposesequations to calculate the stiffness as a function of density of bone tissue such as apparent density and ash density among others[Helgason, Perilli, Schileo, Taddei, Brynjolfsson and Viceconti, 2008]. Other ones present a value of an equivalent elasticity modulus, obtained by statistical adjustments of curves generated through mechanical compression tests over various specimens[Chevalier, Pahr, Allmer, Charlebois and Zysset, 2007; Cuppone, Seedhom, Berry and Ostell, 2004]. Bone tissue is a material withdifferent behaviors according to the scale of observation. It has a complex composite hierarchical structure, which is responsible for assign optimal mechanical properties. Its characteristics, composition and mechanical properties depend on the level at which the material is evaluated[Fritsch and Hellmich, 2007; Hamed, Lee and Jasiuk, 2010]. This paper presents a methodology for computational mechanical simulation of trabecular bones based on the mechanical properties of their elements, hydroxyapatite, type I collagen and non-collagenous proteins with water, and the concentration of these ones obtained by microtomography.

**Keywords:** Microtomography, Trabecular Bone, Properties of Materials, Biomechanics, Computer Simulation, Finite Elements.

## 1 Introduction

Bone is a highly specialized form of conjunctive tissue whose function is to support the higher vertebrates. It is a complex living tissue in which the extracellular matrix is mineralized, providing rigidity and strength to the skeleton, but maintaining certain degree of elasticity. Its composition can be separated into an organic

---

[1] PPGMNE, UFPR, Polytechnic Center - CESEC, Curitiba, Parana, Brazil.
[2] Department of Odontology, PUC, Curitiba, Parana, Brazil.
[3] Vita Hospital, BR 116, Curitiba, Parana, Brazil.
[4] Civil Engineering, UFPR, Polytechnic Center - CESEC, Curitiba, Parana, Brazil.
[5] Civil Construction Department, UFPR, CESEC, Curitiba, Parana, Brazil.

matrix, composed almost entirely of collagen, and an inorganic matrix, composed primarily of calcium and phosphate in the form of hydroxyapatite[Bilezikian, Raisz and Rodan, 1996]. Hydroxyapatite $(Ca_5(PO_4)_6OH)$ is responsible for the stiffness of bone tissue and the fibers of type I collagen by its elasticity[Behari, 2009]. The trabecular bone, object of study of this article, in its composition in microscale, is characterized by a bone matrix formed by lamellae and lacunae, composed by specialized cells such as osteoblasts (bone formation), osteoclasts (bone resorption) and osteocytes. At nanoscale, bone tissue is composed primarily of fibrous type I collagen (tropocollagen) that interact with molecules of hydroxyapatite in an aqueous medium in presence of non-collagenous proteins (NCP).

The ability to simulate the internal structure of a bone in microscale may suggest an improvement in surgical techniques, for example, knee arthroscopy, which is now commonly done to treat the damaged meniscus cartilage, the construction of full prosthesis knee, anterior cruciate ligament reconstruction or treatment of cartilage microfractures, among others. In some of these cases, it is necessary to implant pins or screws for fixation. The identification of mechanical properties of bone tissue of each patient can help, for example, in choosing the best type of screw for each specific case, improving both the surgical procedure and postoperative morbidity. In addition, the proposed model can assist in the development of equipment and tooling systems for surgery applied to the trabecular bone tissue.

In the literature, within the area of biomechanics and bioengineering, it is possible to find works that proposes ways to characterize the bone tissue, mainly seeking tounderstand its mechanical properties.Some authors have presented values of the elastic modulus for human bone tissue[Cuppone, Seedhom, Berry and Ostell, 2004], [Chevalier, Pahr, Allmer, Charlebois and Zysset, 2007], [Uchiyama, Tanizawa, Muramatsu, Endo, Takahashi and Hara, 1999], equine[Leahy, Smith, Easton, Kawcak, Eickhoff, Shetye and Puttlitz, 2010], swine[Teo, Si-Hoe, Keh and Teoh, 2006], muridae[Cory, Nazarian, Entezari, Vartanians, Muller and Snyder, 2010], through destructive tests on reference volumes of bone samples with statistically significant amounts, and some of them also considered samples extracted in many directions for tests[Mittra, Rubin and Qin, 2005], [Ohman, Baleani, Perilli, Dall'Ara, Tassani, Baruffaldi and Viceconti, 2007]. This methodology provides aindication of the samples mechanical properties, applicable with accuracy only over these samples, and providing an approximation to estimated the properties in other different trabecular bones. Other authors presented equations for calculating the elasticity modulus based onbone volume ratio, tissue volume[Guo and Kim, 2002]and bone tissue density in a representative reference volume [Helgason, Perilli, Schileo, Taddei, Brynjolfsson and Viceconti, 2008], [Rho, Hobatho and Ashman, 1995], [Zannoni, Mantovani and Viceconti, 1998], including relations for

elastic modulus obtained for tension and for compression[Kaneko, Pejcic, Tehran-zadeh and Keyak, 2003]. Some of these equations for the trabecular bone tissue were reviewed by Helgason, 2008 [Helgason, Perilli, Schileo, Taddei, Brynjolfsson and Viceconti, 2008] for apparent density, ash density and bone volume fraction. This review shows both the lack of standardized testing and the variation of results. In a certain way, these equations can describe an elastic modulus for bone tissue. The problem is that these equations are very varied and different, depending on the location from where the tissue was extracted and type of bone density. Even using the same kind of density and a very same location to extract a sample in order to proceed the calculation, the equations differ from each other. The test condition and size of the specimen theoretically should not influence the determination of a relationship between density and elastic modulus. However, as each sample is a single chaotic structure it is impossible to obtain a constant ratio[Helgason, Perilli, Schileo, Taddei, Brynjolfsson and Viceconti, 2008]. There are also other authors who presented methods that treat the bone as a material with composite structure and organized in several levels[Rho, Kuhn-Spearing and Zioupos, 1998]. This was made as a way to understand the molecular properties of its elemental constituents in order to describe the mechanical behavior in these various levels or scales[Hamed, Lee and Jasiuk, 2010]using techniques of homogenization and multiscale[Hollister, Brennan and Kikuchi, 1994], [Aoubiza, Crolet and Meunier, 1996].

In fact, bone is a material that behaves according to the scale ofobservation since it has a complex composite hierarchical structure responsible for its optimal mechanical properties. The characteristics, composition and mechanical properties of a bonedepends on the level in which the material is evaluated[Ghanbari and Naghdabadi, 2009; Norman, Shapter, Short, Smith and Fazzalari, 2008; Rho, Kuhn-Spearing and Zioupos, 1998]. Moreover, all these material structures work together to produce the global properties of bone (mechanical, chemical, etc.)[Sansalone, Lemaire and Naili, 2007].The hierarchical structure of bone tissue, starting from the elemental constituents, can be composed as follows: first, entry level, there are collagen fibers in an aqueous medium in the presence of non-collagenous proteins. The next level is represented by the fibers of interfibrillar collagen containing hydroxyapatite crystals, thus, producing mineralized collagen fibers. In the following level, the mineralized collagen fibers are surrounded by a matrix of extrafibrilar hydroxyapatite, consisting of hydroxyapatite in an aqueous medium in the presence of non-collagenous proteins. The final level, addressed in this article, is the level where the mineralized collagen fibers in a matrix of extrafibrilar hydroxyapatite join together, leaving some empty spaces, known as lacunae, to form a single lamellae[Jasiuk and Ostoja-Starzewski, 2004; Nikolov and Raabe, 2008; Sansa-

lone, Lemaire and Naili, 2007]. A model in visiblescale, in this case microscale, which represents satisfactorily the mechanical properties of a bone, should consider all levels of its hierarchical structure[Sansalone, Lemaire and Naili, 2007]studying at each scale which properties are governed by the structural organization at lower levels[Weiner and Traub, 1992].

This paper presents a methodology for computer simulation for the mechanical behavior ofspecific trabecular bone samples, starting from the mechanical properties of the elementary constituents of bone tissue, hydroxyapatite, type I collagen and other, existing at the nanometric level, and its concentration in bone tissue, given by the gray level ofmicrotomography transverse slices and an estimation of the variation in volume fraction of each constituent, based on minimum and maximum values from the literature.

## 2    Description of the method

The bone tissue is a living material and therefore its mechanical properties are functions of numerous biological variables as quantity of certain hormones, biomechanical variables such as physical exercises that the individual undergoes, and physical variables, as the bone density that are different in each individual [Compston, Mellish, Croucher, Newcombe and Garrahan, 1989]. The analysis of the material presented in this article is restricted to a bone tissue of a person with certain characteristics of life, at the very instant when the regeneration and reabsorption functions ceased, what is marked by the time of the sample extraction. The tissue properties degradation was minimized in order to make the acquisition of $\mu$CT images and mechanical tests reveal the original properties of the extracted bone.

### 2.1    *Trabecular bonesamples*

Samples of autologous and homologous human tissue are used for analysis. Its use is approved by the Ethics Committee in Research of the National Health Council, case number 285/2011, which deals with the partnership between the Group of Bioengineering, Federal University of Parana and VitaHospital. Patients who agreed to participate in research, through the donation of residual bone of the tibia after surgery, signed a consent form. The surplus graft or bone piece is recorded, packaged and sent with a registration number that identifies the patient. The medic in charge is the only one with access to the patient's identification. Patient's identity is not revealed in any step of the study.

Samples were taken from surgical discards of human tibia removed during surgical procedures on the knee with variable sizes and shapes. These samples were prepared using a trephine drill (Drill Trephine, Neodent, Curitiba - PR - Brazil)

and a diamondwafering blade (Diamonds Wafering Blades, Buehler, Lake Bluff - Illimois – USA) for precise cutting, to convert the sample into a cylinder of 5 mm diameterand 13 mm height,keeping the ends of the cylinder parallel. After shaping, the samples were submitted to ultrasound (Ultrasound Bath Cleaning - Q335D, QUIMIS ®, Diadema - SP - Brazil) for cleaning inside. The minimization of the degradation of its properties is done by keeping the samples in a saturated 0.9% solution of sodium chloride, that also maintains the osmotic balance. A total of three samples of trabecular bone were used.



**T1**  **T2**  **T3**
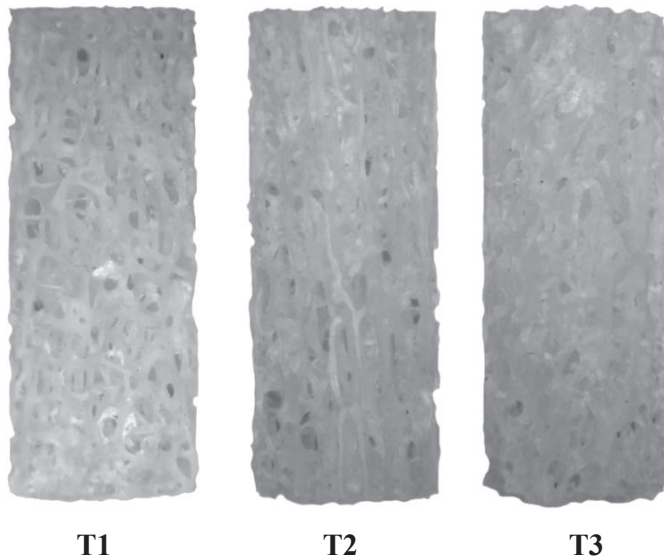
Figure 1: Samples T1, T2 and T3 of trabecular bone seen with 10x magnification.

After tests, samples are packed in plastic material used for medical waste, being returned to the hospital of origin for proper disposal.

## 2.2 Microtomography

After preparation, the samples are submitted to microtomography for the acquisition of transverse $\mu$CT slices that are used both for construction of the three-dimensional geometry of the sample and to obtain the volume fraction of the composite material formed in the microscale level.

### 2.2.1    Aquisition and Reconstruction of μCT Slices

The device used to acquire microtomography was the SkyScan 1172 high resolution (®Skyscan, Kontich - Belgium). The acquisition of radiological images for each sample was made using 80 kV (kilovolt) of power and 124 mA (microamperes) current flow with aluminum 0.5 mm (millimeters)filtering and a exposure time of 6 s (seconds) to eachrotation step of $0.42007°$ for a total of $360°$, resulting in 857 images. The sample was positioned at a distance of 166.51 mm from the X-ray source, ensuring an accuracy of 5.25 micrometers (micron) for each side for each basic unit of the digital image, the pixel, after the reconstruction of tomographic slices.

The reconstruction of transverse slices of the samples is done by a modified Feldkamp algorithm and four computers connected in parallel for data processing, using the reconstruction program NRecon (®Skyscan, Kontich - Belgium), version 1.6.3.0. The results are digital images with resolution of 1360 x 1360 pixels, with a total amount of 2572 images representing cross sections of the bone sample along the height. After the reconstruction, algorithms are applied for cleaning images, removing noise and defects that arise from errors during the process of acquisition and reconstruction, such as ring artifacts or beam hardening.

### 2.2.2    Segmentation and Generation of a representative three-dimensionalgeometric model

Segmentation of μCT transverse slices is a process in which the pixelscorresponding to the bone tissue are selected from images and identified to be used in the generation of a representative three-dimensional geometric model. This procedure is done through the software ScanIP (Simpleware ®, Innovation Centre, Exeter, United Kingdom) generating three-dimensional solidsthat describe the geometric structure of the trabecular bone sample. Figure 2 illustrates the representative three-dimensional geometric model generated throughScanIP for a sample of trabecular bone.

From the representative three-dimensional geometric model described in the STL format is possible to generate a tetrahedral finite element mesh for stress analysis.

### 2.2.3    Finite Elements Discretization

The discretization in finite element mesh of three-dimensional geometry was done using the software Amira®(Visage Imaging, Inc. San Diego, CA, USA). Fig. 3 shows a view of the samples after the generation of finite element mesh.

The finite element meshes of bone samples were generated to have an average of 3.3 million elements.This value was found through the extrapolation of the total
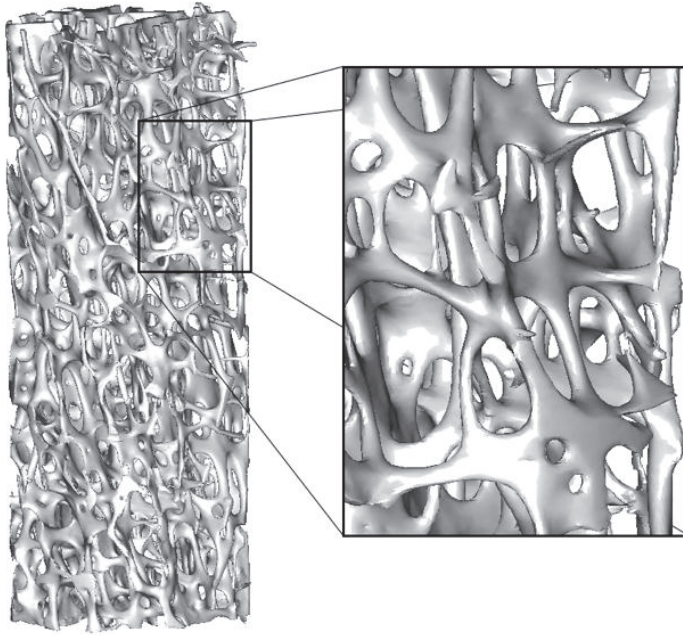
Figure 2: Representative three-dimensional geometric model.

number of elements needed, according to a convergence test over a piece of trabecular bone, to the entire trabecular volume.

Table 1: Properties of finite element meshes.

|  | T1 | T2 | T3 |
|---|---|---|---|
| Number of Nodes | 5.415.234 | 5.051.599 | 5.324.874 |
| Degrees of Freedom | 16.245.702 | 15.154.797 | 15.974.622 |
| Number of Elements | 3.431.572 | 3.134.052 | 3.350.539 |

### 2.2.4 Mechanical Tests

After the acquisition of tomographic images, trabecular bone samples are subjected toa mechanical compression test[Turner and Burr, 1993], Fig. 4. The mechanical tests were performed using a universal testing machine DL10.000, electromechanical microprocessed EMIC (EMIC - Equipment and Systems Testing Ltd.), programmed by a script using TestScript language to implement automated testing. A
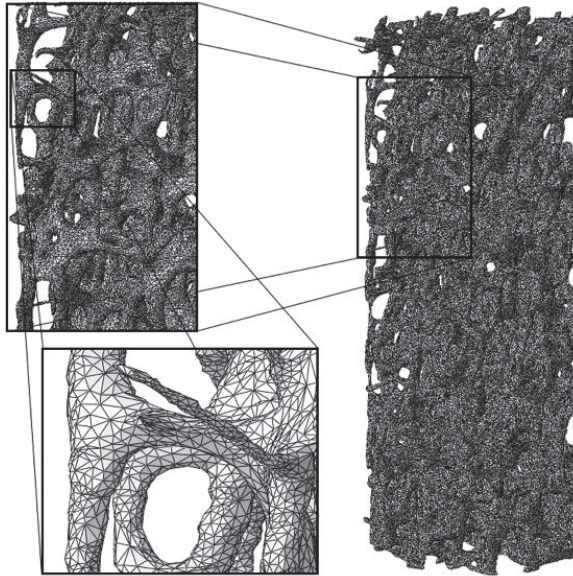
Figure 3: Bone sample discretized finite element.

load cell with maximum capacity of 50 kg was used for the load acquisition. In the test script were set a test speed of 0.01 mm/min, a total displacement of 3 mm andthe detection of material rupture preset to finish the test with 40% of rupture detected. With this results the global mechanical properties of the sample can be evaluated [Fyhrie and Kimura, 1999].
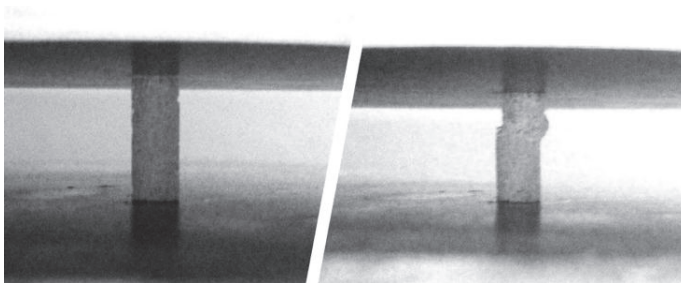


Figure 4: Execution of the compression test.

### 2.2.5   *Homogenization at each hierarchical level*

The hierarchical structure of bone tissue, discussed in this article, consists of four distinct levels, namely: nanoscale, supernanoescale, submicroescale and microscale. It is considered that, at each level, the material has two distinct phases, a matrix and inclusions. The shape of the inclusions is determined by an approximation of its actual format in to a geometric form expressed mathematically. Furthermore, the inclusions must be much smaller than the matrix. Thus, at each hierarchical level inclusions are defined as being formed by the existing structures at lower levels, considering these structures as embedded in a matrix composed of the most abundant material in referenced level.

The homogenization of the phases is made at each level in order to obtain the effective stiffness tensor, which represents the equivalent mechanical behavior of the composite. The main method employed for the homogenization procedure was Mori-Tanaka method. The method was applied at each level in a similar way. The effective stiffness tensor of the level in question is used at the next level for the inclusions and so on until the final level.

According to the hierarchical structure of bone tissue[Weiner and Traub, 1992]defined for this work, the homogenization steps performed at each level are:

1. Nanoscale level, first homogenization: water (matrix) and non-collagenous proteins (inclusions), leading to the aqueous medium;

2. Nanoscale level, second homogenization: collagen fibers (matrix) and the aqueous medium (inclusions), leading to wet collagen fibers;

3. Supernanoescalelevel, first homogenization, wet collagen fibers (matrix) and interfibrillar hydroxyapatite crystals (inclusions), generating mineralized collagen fibers;

4. Supernanoescalelevel, second homogenization: extrafibrilar hydroxyapatite (matrix) and the aqueous medium (inclusions), generating wet extrafibrilarhydroxyapatite;

5. Submicroescalelevel: wet extrafibrilar hydroxyapatite (matrix) and mineralized collagen fibers (inclusions), leading to lamellae matrix;

6. Microscale Level: lamellae matrix (matrix) and lacunae (inclusions), generating a single lamella.

In the final level, the relationship between the single lamellae and lacunae is a function of volume fraction of both constituents, as it is done in all other levels, but

with these fractions calculated according to the gray value from the $\mu$CT transverse slices. Through this, the effective stiffness tensor, in microscale, specific to the trabecular bone sample under analysis is obtained.

The Mori-Tanaka method was chosen for the homogenization of the properties of the composites formed at each hierarchical level of bone tissue, precisely because of their use for this purpose[Fritsch and Hellmich, 2007], [Hamed, Lee and Jasiuk, 2010]. Moreover, the values that the method provides are coherent for the homogenization of composites mechanical properties[Klusemann and Svendsen, 2010].

The Mori-Tanaka method [Mori and Tanaka, 1973] uses the Eshelby equivalent inclusion method [Eshelby, 1957] and the fact that the average deformation in a ellipsoidal matrix circumscribed to an ellipsoidal inclusion is also zero. In addition, the method approximates the interaction between the phases of the composite assuming that each inclusion $i$ is incorporated, at a time, in an infinite matrix which is subject to a uniform load applied away from the inclusion, resulting in a field of average stresses and strains in the matrix $\sigma_M$ and $\varepsilon_M$, respectively[Mura, 1993]. Therefore, the deformation in a simple inclusion $i$ is calculated by,

$$\varepsilon_i = \mathscr{A}_i \varepsilon_M \tag{1}$$

where, $\mathscr{A}_i$ is the influence tensor for a single inclusion[Klusemann and Svendsen, 2010]. The influence tensor can be given by,

$$\mathscr{A}_i = \left[ I + E C_M^{-1} (C_i - C_M) \right]^{-1} \tag{2}$$

being, $I$ the fourth order identity tensor, $E$ Eshelby tensor for an inclusion, depending on the elastic properties of the matrix and the shape of inclusions, $C_i$ the inclusion stiffness tensor and $C_M$ the matrix stiffness tensor[Klusemann and Svendsen, 2010].

Eq. (2) is defined, according Mura, 1993, in the case of ellipsoidal inclusions for a single inclusion[Mura, 1993]. The shapes of inclusions as spherical, cylindrical, ellipsoidal cylinder, can be derived from the ellipsoidal formulation by adjusting the Eshelby tensor, according to the lengths of the axes of the ellipsoid[Mura, 1993]. For example, for a sphere, the axes of the ellipsoid have equal lengths while to a cylinder one axis has an infinite length and so on.

The volume fraction of inclusions and matrix are related as follows[Hamed, Lee and Jasiuk, 2010],

$$f_i + f_M = 1 \tag{3}$$

The effective stiffness tensor for the composite, according to the Mori-Tanaka

method, can be written as[Benveniste, 1987],

$$C_{ef} = C_M + f_i (C_i - C_M) \mathscr{A}_i (f_i \mathscr{A}_i + f_M I)^{-1} \tag{4}$$

This method can be interpreted in the sense that each inclusion behaves like an isolated inclusion in the matrix being $\varepsilon_M$ a far deformationsfield[Benveniste, 1987].

The Eshelby tensor used in Eq. (2) is a fourth-order tensor that relates the eigenstrains, depending on the shape and material of the inclusions, and the matrix, with the total deformation of the composite[Mura, 1993]. If both materials, in the inclusion and in the matrix are isotropic or transversely isotropic materials, the Eshelby tensor has an analytical solution, given respectively by Mura[Mura, 1993] e Li e Dunn[Li and Dunn, 1998].

In the case of the inclusions being in a matrix of anisotropic material, it is necessary to calculate the Eshelby tensor through a numerical method[Klusemann and Svendsen, 2010]. The Eshelby tensor can be calculated by a surface integral, parameterized on the surface of a unit sphere[Mura, 1993], given by,

$$E_{ijkl} = \frac{1}{8\pi} C_{Mijkl} \int_{-1}^{1} \int_{0}^{2\pi} \left[ G_{imjn}\left(\overline{\xi}\right) + G_{jmin}\left(\overline{\xi}\right) \right] d\theta d\overline{\xi}_3 \tag{5}$$

where, $G_{imjn}\left(\overline{\xi}\right)$ is the tensor of Green's functions, derived from the method of Green's functions for the description of eigenstrains[Mura, 1993].

Using the numerical method of Gauss-Legendre integration, the Eq. (5) is rewritten as,

$$E_{ijkl} = \frac{1}{8\pi} C_{Mijkl} \int_{p=1}^{n_p} \int_{q=1}^{n_q} \left[ G_{imjn}\left(\theta_q, \overline{\xi}_{3p}\right) + G_{jmin}\left(\theta_q, \overline{\xi}_{3p}\right) \right] W_q W_p \tag{6}$$

where, $n_p$ isthenumberof Gauss points in direction$\overline{\xi}_3$, $n_q$ thenumberof Gauss points in the angular direction$\theta$, $W_p$ and $W_q$ therespective Gauss weights [Desrumaux, Meraghni and Benzeggagh, 2001].Calculating the Eshelbytensor is possible to calculate the influence tensor of the inclusions and thus find the effective stiffness tensor for the composite.

## 2.2.6 *Volumetric Fractions*

The volumetric fractions in the microscale, are calculated according to the gray level of pixels in the transverse microtomographycslices. All other volumetric fractions, in the other levels are derived from elementary constituents fractions that exists in the single lamellae level (micro) through percentages described in the literature for each elementary constituents[Fritsch and Hellmich, 2007], [Hamed, Lee and Jasiuk, 2010].

The lacunae, its size and quantity in a certain part of the trabecular bone are closely related to bone remodeling, being directly proportional to the osteoclastic activity[Fritsch and Hellmich, 2007], responsible for bone resorption. The size of the lacunae varies with diameters about 0.1 $\mu$m and lengths from 1 to 3 $\mu$m[Jasiuk and Ostoja-Starzewski, 2004]with an approximately ellipsoidal shape. Fractions of these lacunae occur within each voxel[Tkachenko, Slyfield, Tomlinson, Daggett, Wilson and Hernandez, 2009]. These fractions can be identified by the gray value of $\mu$CT transverse slices. Based on the survey of segmentation, where the lower and upper limits of the gray values within bone pieces are found and knowing that the fraction of lacunae inside a cubic voxel size about 5.0 $\mu$m edges may vary about 16% with a variance of 1.9%[Tkachenko, Slyfield, Tomlinson, Daggett, Wilson and Hernandez, 2009] it is possible to create an approximated linear correlation between the gray value of the transverse $\mu$CT images with volume fraction of lamellae matrix for each voxel.
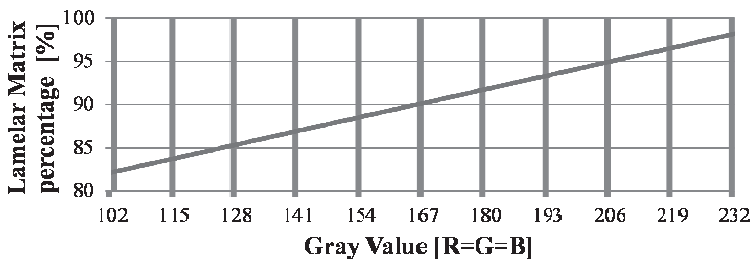


Figure 5: Correlation of the voxel gray value and its corresponding volume fraction of lamellae matrix.

AccordingtoHamedand Lee [Hamed, Lee and Jasiuk, 2010], the volumetric fractions for each elementary constituent of bone tissue present in the lamellae matrix, can be defined keeping the mineral fraction around 50%[Fritsch and Hellmich, 2007].

Table 2: Volume fractions of the elementary constituents for the lamellae matrix [Hamed, Lee and Jasiuk, 2010].

| Constituent | Volumetric Fraction [%] |
|---|---|
| Colagen | 35 |
| Hydroxyapatite | 50 |
| NCP | 5 |
| Water | 10 |

In the lamellae matrix, among the total amount of hydroxyapatite, 25% are from extrafibrilar hydroxyapatite and 75% of interfibrillar hydroxyapatite [Hamed, Lee and Jasiuk, 2010]. In relation to water and non-collagenous protein (NCP), in this paper, the corresponding relations are: 50% come from wet collagen fibers and 50% of wet extrafibrilar hydroxyapatite. 100% of the collagen fibers come from wet collagen. The flowchart in Fig. 6 shows the path of elementary constituents from nanoscale to microscale, being $f_{lm}$ and $f_{lac}$ the volumetric fractions of lamellae matrix and lacunae, given by the graph in Fig. 5 as a function of gray value of the pixel.
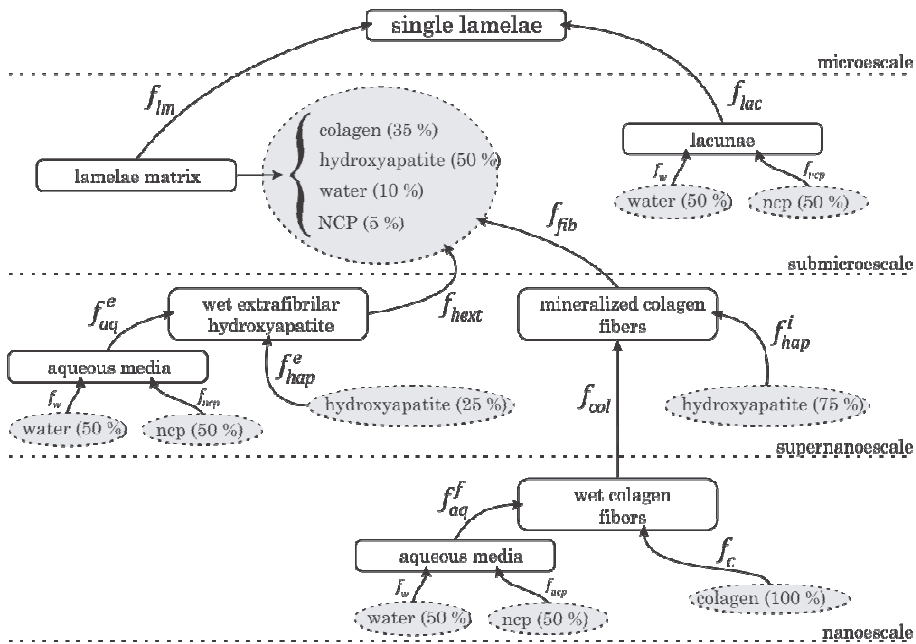


Figure 6: Path of the elementary constituents through the scales.

According to Tab. 2 and Fig 6, the volumetric fractions $f_{fib}$, $f_{hext}$, $f_{aq}^e$, $f_{hap}^e$, $f_{col}$, $f_{hap}^i$, $f_c$, $f_{aq}^f$, $f_w$, $f_{ncp}$ are defined for the mineralized collagen fibers, wet hydroxyapatite matrix, aqueous medium of the wet hydroxyapatite matrix, extrafibrilar hydroxyapatite, wet collagen fibers, interfibrillar hydroxyapatite, collagen fibers, aqueous medium of wet collagen fiber, water and non-collagenous proteins, respectively.

The values of Tab. 3 are defined in this paper in order to maintain the percentages defined in Tab. 2 for the mineral part (hydroxyapatite), organic (collagen) and other

Table 3: Volumetric Fractions Values

| Volumetric Fractions | Value [%] |
|:---:|:---:|
| $f_{fib}$ | 75 |
| $f_{hext}$ | 25 |
| $f_{aq}^e$ | 15 |
| $f_{hap}^e$ | 85 |
| $f_{col}$ | 50 |
| $f_{hap}^i$ | 50 |
| $f_c$ | 85 |
| $f_{aq}^f$ | 15 |
| $f_w$ | 67 |
| $f_{ncp}$ | 33 |

constituents (water and NCP).

### 2.2.7  *Principal Directions*

At each level of homogenization anisotropic fourth-order continuous stiffness tensors are written with the principal directions remaining constant and generic for the homogenization steps[Hamed, Lee and Jasiuk, 2010]. The generalization of the directions is achieved by specifying the same directions for the main elementary constituents, namely: collagen, hydroxyapatite, water and non-collagenous proteins in order to engender the construction of the stiffness tensor.

Because the elongated fiber and crystal shapes of the collagen and hydroxyapatite, they have a specific main direction. In this paper, this direction is defined as identical for both elements in every step of homogenization where thecorresponding elementary stiffness tensors are employed, as in the nanoscale and supernanoescale.

Consideration of an anisotropic continuous matrix is taken based on two main arguments. The first comes from the fact that collagen molecules have the form of triple helix and are connected by cross-linking, which guarantees continuity in the structure[Buehler, 2006]. The second comes from the assumption that the hydroxyapatite crystals have compact form, and strongly adhere to the fiber surface, which again ensures the use of continuous matrix and the application of Mori-Tanaka method in the process of obtaining the tensor of equivalent stiffness[Hamed, Lee and Jasiuk, 2010].

The generalization of the principal directions, based on directions of the elementary constituents is applied to the nanoscale level,supernanoescale and submicroescale. At the microscale level, where there is lamellae matrix with empty spaces known as

lacunae, a different assumption is made for the local axes of each single lamellae represented by a voxel.The equivalent stiffness tensors obtained in this level for each voxel or lamellae, were made considering their principal direction as the same directions of the trabeculae.

A procedure for coordinate transformation of the fourth order tensor, given by Eq. (8), is used to obtain the equivalent stiffness tensor of voxel, written in global directions [Lai, Rubin and Krempl, 2010].

$$C'_{ijkl} = Q_{mi}Q_{nj}Q_{rk}Q_{sl}C_{mnrs} \tag{7}$$

being, $C_{mnrs}$ the equivalent stiffness tensor of voxel obtained by the process of homogenization of Mori-Tanaka for the last hierarchical level, microscale, $Q_{ij}$ the matrix of directive cosines (the transformation matrix between local and global axes) e $C'_{ijkl}$ the equivalent stiffness tensor of the voxel in the total directions.

### 2.2.8 *Anisotropic stiffness tensor of each finite element*

The anisotropic stiffness tensor of each finite element is calculated using the approximation of Voigt[Mura, 1993]. Voigt's method is known from the literature for presenting overestimated values, being used as the upper limit[Hamed, Lee and Jasiuk, 2010]for the analysis of homogenization methods. However, because inside a finite element it is an idealized material (a bunch of piled cubes or voxels), which does not define matrix and inclusions, the method can be applied as a first approach to the problem. The stiffness tensor of each finite element ($C_{elem}$) is calculated from the stiffness tensor calculated for each voxel representing the bone ($C^i_{vox}$), based on the volumetric fractions of each voxel ($f^i_{vox}$) present within the finite element by its respective stiffness tensor.

$$C_{elem} = \int_{i=1}^{n_{ve}} f^i_{vox}C^i_{vox} \tag{8}$$

being, $n_{ve}$ the total number of voxels within the finite element in question.

After proceeding a survey about which voxels are present within each finite element, the Voigt's approximated homogenization method is applied in order to obtain the stiffness tensors for each one of these elements.

The volumetric fractions of each voxel are nothing else than very volume of them. Each voxel has cubic shape with 5,25 $\mu$m edges (function of the microtomography parameters) with a total volume of 144,70 $\mu$m$^3$. The sum of the volumetric fractions of all voxels within certain finite element should be approximately equal to the volume of the same finite element.

### *2.3   Computacional Simulation*

The purpose of the computational simulation was to obtain the force by displacement curve of the finite element model of the trabecular bone samples. The simulation was based on the properties of their elementary constituents, function of volumetric fractions, obtained at the microscale for lamellae and lacunae. To this end, the properties calculated through the homogenization process should be evaluated for each finite element in the model.
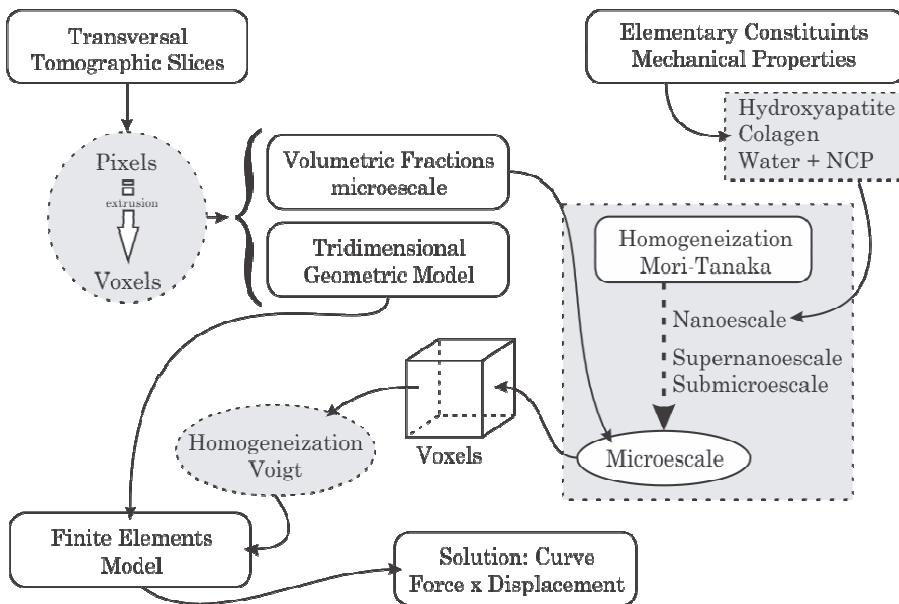


Figure 7: Flowchart for generating the finite element model.

A microscaleeffective tensor, representing a single lamellae is associated with each voxel of the three-dimensional geometric model. This tensor is calculated according to the methodology of multiscale homogenization and according to the volumetric fractions defined by the gray value derived froma transverse microtomography slice.

In the next step, the voxels present within each finite element are determined.A simple homogenization of the properties of each voxel, using the Voigt homogenization scheme is made for calculating the anisotropic stiffness tensor of each finite element. As each sample is around 3.3 million elements and each element receives an anisotropic stiffness tensor, each analysis has approximately 3,300,000

stiffness tensors.

The finite element model is solved through the application of concentrated loads representing a total load of 150 N in the upper nodes of the model, constraining the displacements of the nodes of the upper surface to have equal displacement. Boundary conditions are inserted in the lower nodes, considering them fixed, for the simulation of mechanical testing and obtaining the force by displacement computational curve.

An application in python, divided into modules, was developed for these procedures. The final result of this algorithm is a computer simulation, through the finite element method, of the linear elastic part of the physical mechanical test. The resolution of the computer simulation took about three days for each bone sample and was only possible through the Linux operating system Ubuntu 4.10 LTS (Lucid Lynx) (http://www.ubuntu-br.org/).

The algorithm was written in python, because of the ease implementation and productivity offered by this programming language. After concluding the simulation and obtaining a graphic of force by displacement, the evaluation and comparison of the results contrasting with physical mechanical tests were done.

The calculation of elastic moduli for both physical tests and the results of the computer simulations were made according to the slopes obtained with trend lines for the linear part of the force by displacement curves. These values were calculated as functions of the total height and the cross-sectional area of the samples, according to the Eq. (9).

$$E = I_{FD} \frac{h}{A} \qquad (9)$$

where, $I_{FD}$ trend line slope for the force by displacement graphs, $h$ total height of the samples (13 mm), $A$ the cross-sectional area and $E$ the elastic modulus of the sample.

## 3 Results

Graphics comparing the physical mechanical tests and the computer simulation of the mechanical tests, using finite elements for samples T1, T2 and T3 are shown in Fig. 8. Due to the size and complexity of computer simulation, comparisons are restricted to linear elastic regime.

## 4 Discussion and Conclusions

Bone tissue is a complex material in its geometry, mechanical properties, physical and biological characteristics. The complexity of the issue justifies the numerous
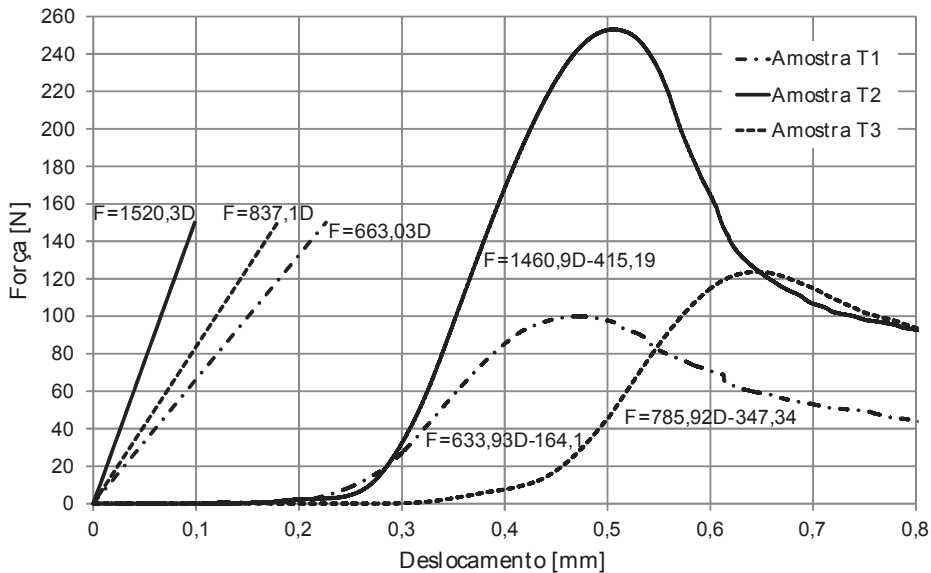
Figure 8: Force vs. Displacement comparison graphic for the sample T1, T2 and T3, respectively.

studies where the main subject is the bone, both cortical and trabecular one. The characteristics studied such as mechanical properties are disparate and almost never define or standardize a generic behavior.

Indeed the mechanical characterization of a bone is almost an impossible mission when adopted an simplified approach since the properties of it are functions of many biological variables as the amount of certain hormones, biomechanical variables such as amount of exercise that a person undergoes and physical variables such as bone density, which one is different in every person atdifferent moments in life. This occurs because bone is a living tissue that undergoes constant damage and recovery (bone remodeling)to the extent of changing the entire human skeleton in approximately eight years[Behari, 2009].

The approach of bone tissue as a composite material consisting of a multiscale hierarchical structure in which, at each level, all the structures compounding the material work together to produce the global properties of the bones (mechanical, chemical, etc.), is currently the most accepted approachproducing the most consistent results. This assertion can be made based on the latest publications on the mechanical behavior of bone tissue[Coelho, Fernandes and Rodrigues, 2011; Hackl, Ilic and Gilbert, 2010; Hambli, 2010; 2011; Hambli, Katerchi and Benhamou,

2011; Hamed, Lee and Jasiuk, 2010; Ilic, Hackl and Gilbert, 2010; Levengood, Po-lak, Wheeler, Maki, Clark, Jamison and Johnson, 2010; Podshivalov, Fischer and Bar-Yoseph, 2011].

However, the mere consideration of bone tissue as a hierarchical and multiscale material does not guarantee the general characterization since it undergoes a high variation in its mechanical properties. The method proposed in this paper for a bet-ter approximation of the real and correct mechanical properties in a specific bone sample is to measure the amounts of bone constituents at a certain level or scale, more specifically, in the microscale, and use these measures in the stiffness tensors formulation. Theses tensors represent the mechanical properties for each represen-tative volume where it is possible to identify certain variation of these properties, being these representative volumes the voxels.

There are many difficulties on implementing a model with these proposed features, starting from the complexity of the multiscale mathematical procedure andhomog-enization, and ending with enormity of the computer model to represent a small sample of 5 mm in diameter and 13 mm in height. The justification for this model liesin the possibility of implementing large computational models due to the lat-est generation of computers available in ordinary consumers market in the years of 2010 and 2011. Also, another justificationis the possibility of using very high level programming languages, as python, what guarantees a high productivity.

A model with this level of complexity can provide much more than a simple com-parison with mechanical compression tests. Its evolution in terms of implementing features as damage, fracture, and other non-linear mechanical theories, can lead to a deeper understanding about bone tissue's behavior and consequently improve the process of computer simulation for these structures. The material damage is visi-ble by observing the displacement-force curve of physical compression tests. For example, the curve for sample T2, Fig. 8, shows the starting point of damage after the linear elastic regime followed by a major loss of rigidity. In the curves, another depicted point deserves some commentaries. This is the point of stiffness initial gain, which can be understood as a failure (and even rupture) of the trabeculae in contact with the surface of the load stage due to the small contact area, which is about 10 to 15% of the total cross-sectional samples. This rupture occurs until the point that the packaging of these fractured trabeculae generates a sufficient con-tact area for the whole sample to be requested and the structure as a whole start to work mechanically. Even so, it is possible to note that the elastic regime is not as linear as it is supposed to be according to the theoretical definition. There is a little damage occurring with this scheme. This damage can be a residue of failure and continuous breaking offin the structures that initially collapsed, or a failure of small trabecular structures, arranged in improper positions in relation to the stress

concentration, what causes a fast elevationin the tension level rapidly achieving the collapse.

Regarding the results obtained through the methodology proposed in this paper, there are discrepancies in the computational results in relation to the physical results, from approximately 4% for samples 1 and 2 and 6% in sample 3. This error maybe a result from several variables involved in development of the employed methodology. It can be related to the application of Voigt's homogenization theory, classically known in the literature for overestimate stiffness values for composites[Hamed, Lee and Jasiuk, 2010], or the occurrence of damage and failure of structures, previously to the linear regime, causing a global behavior distinct from the behavior calculated in the computer modeling. In addition, the methodology itself may need some adjustments. Another factor to be considered is to soak the ends of the bone sample in a resin or similar material to ensure an area of load transfer that does not begin with an early damage on parts of the end structure during the sample's physical compression tests, what makes possible even a tensile test. This approach requires that the contact surface between the resin and the bone must be calculated as well as the mechanical properties of the resin should be known.

The presented methodology for trabecular bone tissue computational simulation was found to be approximately consistent with the results of physical tests. It means that, in a certain way, the methodology can be applied in the prediction of stresses and strains intrabecular bone structures. The main consideration on the proposed methodology is the fact that it can characterize specific trabecular bone structures departing from same values of stiffness tensors for the elementary constituents. This fact is illustrated by the variation in the force displacement graphics of each sample in computer simulations. Being function of microtomography parameters, this characterization is a noninvasive technique that according to some special parameters can even be applied *in vivo*.

Cases in which the methodology is applicable are those ones where there was no damage in the trabecular structure and also when only an idea about the structure behavior in linear elastic regime is needed.

Despite of its limitations, the methodology was found to be efficient on the characterization of specific bone structures, achieving global mechanical properties similar to the same properties evaluated through mechanical testes according to every different samples of human trabecular bones.

Thus, studies in specific locations of certain individual's trabecular bone tissue, with certain characteristics, according to the time when his functions of regeneration and resorption ceased can employ the proposed methodology in order to obtain the structure's response about the stress and strain relation on an elastic regime.

## References

**Aoubiza, B.; J. M. Crolet; A. Meunier** (1996): On the mechanical characterization of compact bone structure using the homogenization theory. *J Biomech*, 29(12), 1539-1547.

**Behari, J.** (Ed.) (2009): *Biophysical bone behavior*, 501 pp., John Wiley & Sons (Asia), Singapore.

**Benveniste, Y.** (1987): A new approach to the application of Mori-Tanaka's theory in composite materials. *Mechanics of Materials*, 6(2), 147-157.

**Bilezikian, J. P.; L. G. Raisz; G. A. Rodan** (1996): *Principles of bone biology*, xx,1398p.,[1316]p. of plates pp., Academic Press, San Diego ; London.

**Buehler, M. J.** (2006): Nature designs tough collagen: Explaining the nanostructure of collagen fibrils. *Proceedings of the National Academy of Sciences*, 103(33), 12285-12290.

**Chevalier, Y.; D. Pahr; H. Allmer; M. Charlebois; P. Zysset** (2007): Validation of a voxel-based FE method for prediction of the uniaxial apparent modulus of human trabecular bone using macroscopic mechanical tests and nanoindentation. *J Biomech*, 40(15), 3333-3340.

**Coelho, P. G.; P. R. Fernandes; H. C. Rodrigues** (2011): Multiscale modeling of bone tissue with surface and permeability control. *J Biomech*, 44(2), 321-329.

**Compston, J. E.; R. W. E. Mellish; P. Croucher; R. Newcombe; N. J. Garrahan** (1989): Structural mechanisms of trabecular bone loss in man. *Bone and Mineral*, 6(3), 339-350.

**Cory, E.; A. Nazarian; V. Entezari; V. Vartanians; R. Muller; B. D. Snyder** (2010): Compressive axial mechanical properties of rat bone as functions of bone volume fraction, apparent density and micro-ct based mineral density. *J Biomech*, 43(5), 953-960.

**Cuppone, M.; B. B. Seedhom; E. Berry; A. E. Ostell** (2004): The longitudinal Young's modulus of cortical bone in the midshaft of human femur and its correlation with CT scanning data. *Calcif Tissue Int*, 74(3), 302-309.

**Desrumaux, F.; F. Meraghni; M. L. Benzeggagh** (2001): Generalised Mori-Tanaka scheme to model anisotropic damage using numerical Eshelby tensor. *J Compos Mater*, 35(7), 603-624.

**Eshelby, J. D.** (1957): The Determination of the Elastic Field of an Ellipsoidal Inclusion, and Related Problems. *Proc R Soc Lon Ser-A*, 241(1226), 376-396.

**Fritsch, A.; C. Hellmich** (2007): 'Universal' microstructural patterns in cortical and trabecular, extracellular and extravascular bone materials: Micromechanics-based prediction of anisotropic elasticity. *J Theor Biol*, 244(4), 597-620.

**Fyhrie, D. P.; J. H. Kimura** (1999): Cancellous bone biomechanics. *J Biomech*, 32(11), 1139-1148.

**Ghanbari, J.; R. Naghdabadi** (2009): Nonlinear hierarchical multiscale modeling of cortical bone considering its nanoscale microstructure. *J Biomech*, 42(10), 1560-1565.

**Guo, X. E.; C. H. Kim** (2002): Mechanical consequence of trabecular bone loss and its treatment: a three-dimensional model simulation. *Bone*, 30(2), 404-411.

**Hackl, K.; S. Ilic; R. Gilbert** (2010): Multiscale modeling for cancellous bone by using shell elements. *Shell Structures: Theory and Applications, Vol 2*, 249-252.

**Hambli, R.** (2010): Application of Neural Networks and Finite Element Computation for Multiscale Simulation of Bone Remodeling. *J Biomech Eng-T Asme*, 132(11), -.

**Hambli, R.** (2011): Multiscale prediction of crack density and crack length accumulation in trabecular bone based on neural networks and finite element simulation. *Int J Numer Meth Bio*, 27(4), 461-475.

**Hambli, R.; H. Katerchi; C. L. Benhamou** (2011): Multiscale methodology for bone remodelling simulation using coupled finite element and neural network computation. *Biomech Model Mechan*, 10(1), 133-145.

**Hamed, E.; Y. Lee; I. Jasiuk** (2010): Multiscale modeling of elastic properties of cortical bone. *Acta Mech*, 213(1-2), 131-154.

**Helgason, B.; E. Perilli; E. Schileo; F. Taddei; S. Brynjolfsson; M. Viceconti** (2008): Mathematical relationships between bone density and mechanical properties: A literature review. *Clin Biomech*, 23(2), 135-146.

**Hollister, S. J.; J. M. Brennan; N. Kikuchi** (1994): A homogenization sampling procedure for calculating trabecular bone effective stiffness and tissue level stress. *J Biomech*, 27(4), 433-444.

**Ilic, S.; K. Hackl; R. Gilbert** (2010): Application of the multiscale FEM to the modeling of cancellous bone. *Biomech Model Mechan*, 9(1), 87-102.

**Jasiuk, I.; M. Ostoja-Starzewski** (2004): Modeling of bone at a single lamella level. *Biomech Model Mechan*, 3(2), 67-74.

**Kaneko, T. S.; M. R. Pejcic; J. Tehranzadeh; J. H. Keyak** (2003): Relationships between material properties and CT scan data of cortical bone with and without metastatic lesions. *Med Eng Phys*, 25(6), 445-454.

**Klusemann, B.; B. Svendsen** (2010): Homogenization methods for multi-phase elastic composites: Comparisons and Benchmarks. *Technische Mechanik*, (4), 374-386.

**Lai, W. M.; D. Rubin; E. Krempl** (2010): *Introduction to continuum mechanics*. 4th ed., xiv, 520 p. pp., Butterworth-Heinemann/Elsevier, Amsterdam; Boston.

**Leahy, P. D.; B. S. Smith; K. L. Easton; C. E. Kawcak; J. C. Eickhoff; S. S. Shetye; C. M. Puttlitz** (2010): Correlation of mechanical properties within the equine third metacarpal with trabecular bending and multi-density micro-computed tomography data. *Bone*, 46(4), 1108-1113.

**Levengood, S. K. L.; S. J. Polak; M. B. Wheeler; A. J. Maki; S. G. Clark; R. D. Jamison; A. J. W. Johnson** (2010): Multiscale osteointegration as a new paradigm for the design of calcium phosphate scaffolds for bone regeneration. *Biomaterials*, 31(13), 3552-3563.

**Li, J. N. Y.; M. L. Dunn** (1998): Anisotropic coupled-field inclusion and inhomogeneity problems. *Philos Mag A*, 77(5), 1341-1350.

**Mittra, E.; C. Rubin; Y. X. Qin** (2005): Interrelationship of trabecular mechanical and microstructural properties in sheep trabecular bone. *J Biomech*, 38(6), 1229-1237.

**Mori, T.; K. Tanaka** (1973): Average Stress in Matrix and Average Elastic Energy of Materials with Misfitting Inclusions. *Acta Metall Mater*, 21(5), 571-574.

**Mura, T.** (1993): *Micromechanics of defects in solids*. 2nd, rev. ed. ed., XIII-587 pp., Kluwer Academic publ., Dordrecht Boston London.

**Nikolov, S.; D. Raabe** (2008): Hierarchical modeling of the elastic properties of bone at submicron scales: The role of extrafibrillar mineralization. *Biophys J*, 94(11), 4220-4232.

**Norman, J.; J. G. Shapter; K. Short; L. J. Smith; N. L. Fazzalari** (2008): Micromechanical properties of human trabecular bone: a hierarchical investigation using nanoindentation. *J Biomed Mater Res A*, 87(1), 196-202.

**Ohman, C.; M. Baleani; E. Perilli; E. Dall'Ara; S. Tassani; F. Baruffaldi; M. Viceconti** (2007): Mechanical testing of cancellous bone from the femoral head: Experimental errors due to off-axis measurements. *J Biomech*, 40(11), 2426-2433.

**Podshivalov, L.; A. Fischer; P. Z. Bar-Yoseph** (2011): 3D hierarchical geometric

modeling and multiscale FE analysis as a base for individualized medical diagnosis of bone structure. *Bone*, 48(4), 693-703.

**Rho, J. Y.; M. C. Hobatho; R. B. Ashman** (1995): Relations of Mechanical-Properties to Density and Ct Numbers in Human Bone. *Med Eng Phys*, 17(5), 347-355.

**Rho, J. Y.; L. Kuhn-Spearing; P. Zioupos** (1998): Mechanical properties and the hierarchical structure of bone. *Med Eng Phys*, 20(2), 92-102.

**Sansalone, V.; T. Lemaire; S. Naili** (2007): Multiscale modelling of mechanical properties of bone: study at the fibrillar scale. *Cr Mecanique*, 335(8), 436-442.

**Teo, J. C. M.; K. M. Si-Hoe; J. E. L. Keh; S. H. Teoh** (2006): Relationship between CT intensity, micro-architecture and mechanical properties of porcine vertebral cancellous bone. *Clin Biomech*, 21(3), 235-244.

**Tkachenko, E. V.; C. R. Slyfield; R. E. Tomlinson; J. R. Daggett; D. L. Wilson; C. J. Hernandez** (2009): Voxel size and measures of individual resorption cavities in three-dimensional images of cancellous bone. *Bone*, 45(3), 487-492.

**Turner, C. H.; D. B. Burr** (1993): Basic biomechanical measurements of bone: A tutorial. *Bone*, 14(4), 595-608.

**Uchiyama, T.; T. Tanizawa; H. Muramatsu; N. Endo; H. E. Takahashi; T. Hara** (1999): Three-dimensional microstructural analysis of human trabecular bone in relation to its mechanical properties. *Bone*, 25(4), 487-491.

**Weiner, S.; W. Traub** (1992): Bone structure: from angstroms to microns. *FASEB J*, 6(3), 879-885.

**Zannoni, C.; R. Mantovani; M. Viceconti** (1998): Material properties assignment to finite element models of bone structures: a new method. *Med Eng Phys*, 20(10), 735-740.